Redox Biology 20 (2019) 307–320

Contents lists available at ScienceDirect

Redox Biology

journal homepage: www.elsevier.com/locate/redox

MnSOD is implicated in accelerated wound healing upon Negative Pressure Wound Therapy (NPWT): A case in point for MnSOD mimetics as adjuvants for wound management

Gregory Lucien Bellot[a,b], Xiaoke Dong[a], Amitabha Lahiri[a], Sandeep Jacob Sebastin[a], Ines Batinic-Haberle[d], Shazib Pervaiz[b,c,e,f,g,*], Mark Edward Puhaindran[a,**]

[a] Department of Hand & Reconstructive Microsurgery, University Orthopedic, Hand & Reconstructive Microsurgery Cluster, National University Health System, Singapore
[b] Department of Physiology, Yong Loo Lin School of Medicine, National University of Singapore, Singapore
[c] Medical Science Cluster Cancer Program, Yong Loo Lin School of Medicine, National University of Singapore, Singapore
[d] Department of Radiation Oncology, Duke University School of Medicine, Durham, NC, USA
[e] National University Cancer Institute, National University Health System, Singapore, Singapore
[f] NUS Graduate School for Integrative Sciences and Engineering, National University of Singapore, Singapore
[g] School of Pharmacy and Biomedical Sciences, Curtin University, Perth, Australia

ARTICLE INFO

Keywords:
Negative pressure wound therapy
Skin wound healing
Manganese superoxide dismutase
MnSOD mimetics
MnTE-2-PyP^{5+}

ABSTRACT

Negative Pressure Wound Therapy (NPWT), a widely used modality in the management of surgical and trauma wounds, offers clear benefits over conventional wound healing strategies. Despite the wide-ranging effects ascribed to NPWT, the precise molecular mechanisms underlying the accelerated healing supported by NPWT remains poorly understood. Notably, cellular redox status-a product of the balance between cellular reactive oxygen species (ROS) production and anti-oxidant defense systems-plays an important role in wound healing and dysregulation of redox homeostasis has a profound effect on wound healing. Here we investigated potential links between the use of NPWT and the regulation of antioxidant mechanisms. Using patient samples and a rodent model of acute injury, we observed a significant accumulation of MnSOD protein as well as higher enzymatic activity in tissues upon NPWT. As a proof of concept and to outline the important role of SOD activity in wound healing, we replaced NPWT by the topical application of a MnSOD mimetic, Mn(III) *meso*-tetrakis(*N*-ethylpyridinium-2-yl)porphyrin (MnTE-2-PyP^{5+}, MnE, BMX-010, AEOl10113) in the rodent model. We observed that MnE is a potent wound healing enhancer as it appears to facilitate the formation of new tissue within the wound bed and consequently advances wound closure by two days, compared to the non-treated animals. Taken together, these results show for the first time a link between NPWT and regulation of antioxidant mechanism through the maintenance of MnSOD activity. Additionally this discovery outlined the potential role of MnSOD mimetics as topical agents enhancing wound healing.

1. Introduction

Management of acute and chronic wounds is one of the important clinical challenges faced by modern societies [1]. The increasing incidence of diseases such as diabetes and peripheral vascular disease, coupled with an aging population, are likely to be associated with an increase in non-healing and chronic wounds, which can lead to severe consequences such as limb amputations or untimely deaths [2]. Wound management already represents a significant economic burden on healthcare systems, which is expected to increase significantly due in part to better life expectancy, and therefore, the probability of prolonged care for chronic diseases that amplify the risk for acute and/or chronic wounds. As such, there is a heightened realization to design better and effective therapeutic strategies in order to achieve more optimized and efficient wound healing [3,4].

Skin wound healing is a complex physiological process that results in tissue repair and regeneration. It is organized into four major and overlapping phases: haemostasis, inflammation, proliferation and remodelling [5–8]. Haemostasis begins as soon as the tissue is damaged, and is achieved through platelet plugging and fibrin matrix formation.

* Corresponding author at: Department of Physiology, Yong Loo Lin School of Medicine, National University of Singapore, Singapore.
** Corresponding author.
E-mail addresses: phssp@nus.edu.sg (S. Pervaiz), mark_e_puhaindran@nuhs.edu.sg (M.E. Puhaindran).

https://doi.org/10.1016/j.redox.2018.10.014
Received 19 June 2018; Received in revised form 30 September 2018; Accepted 17 October 2018
Available online 23 October 2018

This is followed by neutrophil recruitment, which marks the start of the inflammatory stage. The second phase of inflammation occurs around 48 h following injury and is characterized by monocyte recruitment and differentiation into macrophages, clearing the wound site and coordinating the later stages of wound healing through cytokine production [8–10]. The proliferation phase is associated with the formation of new tissue to replace the fibrin matrix to facilitate scar formation and closure of the wound: this is mostly achieved through fibroblast migration, restoration of vascularization (angiogenesis), granulation tissue formation (fibroblasts, new blood capillaries and macrophages) and keratinocyte migration on the upper layer of granulation tissue [5,7,8]. Some fibroblasts then undergo differentiation into myofibroblasts, which are involved in wound contraction, bringing the wound edges together. The remodelling phase involves the removal of cells recruited to the wound in the previous stages through apoptosis, and restoration of the collagen structure [7]. The underlying mechanisms involved in the wound healing process(es) as well as the factors that regulate and/or impede the cellular responses are complex and not fully understood [6,11]. Therefore, despite the huge advances in medicine in the last century, improvements in wound care and management have occurred at a much slower pace [11,12]. The therapeutic efficacy of adjuncts in wound healing has been reported; however, the overall benefits of most techniques have been marginal.

NPWT is a modality that has shown great promise [13,14] and delivered significantly better results in the clinical care of acute as well as chronic wounds, such as diabetic foot ulcers [6,15–17]. It is designed to seal the wound site using foam dressing linked to an electronic pump, which applies a pressure ranging from − 75 to − 125 mmHg. As a matter of fact, NPWT's impact on wound healing appears to be the consequence of multiple effects, each contributing to the overall positive influence on wound healing. More interestingly, the sum of these effects makes NPWT a suitable tool to treat diverse type of wounds such as surgical wounds, acute open wounds or chronic wounds, as it positively influences the various parameters that affect the healing of diverse types of wounds [13,18,19]. Among the described positive effects of NPWT are an improvement in blood irrigation of the wound site associated with enhanced angiogenesis [20–22]. The impact on angiogenesis appears to occur through an increase in VEGF and a modulation of hypoxia response and signaling across the wound [21–24]. The improvement in perfusion is associated with micro-deformation mechanisms linked to enhanced proliferation and formation of granulation tissue, which is a characteristic of NPWT [13,22,25]. The type of mechanical effect triggered by NPWT called microdeformation is the product of the interface created between the wound bed and the wound filler [26]. This effect has been correlated with an improved blood perfusion, angiogenesis and cell proliferation [20,22,27,28]. Though poorly understood it was shown to stimulate bFGF (basic Fibroblast Growth Factor) and the downstream activation of ERK1/2 indicating cell proliferation stimulated through MAPK pathway [28,29]. Also microdeformation promotes angiogenesis and vascular remodelling through upregulation of VEGF (Vascular Endothelial Growth Factor) which is critical in the elongation and proliferation of endothelial cells but also plays an important role in the regulation of inflammation [22,29,30]. Blood flow measurements reinforced the important impact of NPWT in neo-vascularization showing about a five times increase three days after its application [21]. Based on these studies it appears that angiogenesis stimulated by negative pressure therapy is a critical mechanism by which wound healing is promoted and an important parameter in the granulation tissue formation which is characteristic of NPWT treatment.

Additionally, macro-deformation on the wound edges has been associated with oedema reduction and decrease of the wound area through application of compressive forces associated with a suction mechanism that generates contractile forces [31,32]. Finally, NPWT has been shown to control exudates by clearing excess fluids and has been associated with a decrease in bacterial load, thus potentially decreasing wound infection risks [13].

While the clinical benefits of NPWT are well documented, the underlying mechanisms that promote the process of wound healing remain poorly understood [13,25,33]. There is strong evidence linking molecular oxygen, ROS production and cellular antioxidant defense systems to the different stages of wound healing [34–38]. Indeed, ROS is involved during the inflammation and angiogenesis phases, and elicit protective activity against pathogens [34,36]. Variations of antioxidant enzymes activities in skin wounds such as catalase, superoxide dismutase 1 & 2 (SOD 1 and 2), glutathione peroxidase and peroxiredoxins have been described in different models [34]. SOD1 knockout mice exhibit skin damage and impaired wound healing. In addition, expression levels and/or activities of some of these redox modifying enzymes have been shown to be reduced in diabetes, which is associated with impaired wound healing [36,39]. It is noteworthy that many natural compounds that have been reported to improve wound healing exhibit some antioxidant properties [37,40,41].

In this study we tested the hypothesis that NPWT may impact redox homeostasis of the wound through the modulation of antioxidant mechanisms. Using a rodent model of acute wound induction as well as tissues derived from patients, we provide evidence that NPWT predominantly affects SOD activity, in particular SOD2. We then postulated that the effects of NPWT could be partially recapitulated by the use of a topical SOD2 mimetic (MnTE-2PyP^{5+}; MnE). MnE has been shown to distribute preferentially in mitochondria, both in *Saccharomyces cerevisiae* and in mice [42–44], and is currently undergoing clinical evaluation for the treatment of atopical dermatitis and itch, hence the justification for its utility in wound healing. Indeed, we provide evidence that topical application of MnE accelerates and promotes the process of wound healing in the rodent acute wound model, thus highlighting a novel application of SOD2 mimetics in wound therapy.

2. Material and methods

2.1. Collection of patient-derived tissue

This study was approved by the Institutional Review Board of Singapore (Ref n° 2012/00251). Skin subcutaneous fat and fascia samples were obtained from surgically removed tissue. The tissue was surgically debrided from the acute wounds of patients following trauma, after which Negative Pressure Wound Therapy (NPWT) dressings were applied. Surgery was performed at the time of injury, and at varying durations for follow up wound debridement and dressing change, before definitive wound coverage or closure was performed. All surgical procedures performed were part of the clinical care. The harvested tissue was subsequently snap frozen in liquid nitrogen before processing for biochemical analysis.

2.2. Rodent injury model

The protocols used in this study were approved and validated by the IACUC (protocol R14–476) and were adapted from a previously published model [14]. For the rats treated with Negative Pressure apparatus, on day 1 and after anaesthesia with isoflurane, the back of the rats were shaved and prepped with betadine. A 2*2 cm full thickness wound was then created on the dorsa of the animals. The animals were divided into 2 groups: a control group which received NPWT dressing without suction and an experimental group of rats receiving the standard NPWT dressing subjected to negative 125 mmHg of continuous pressure for 4 days. The dressing in both groups was changed every 2 days and the wound cleaned (after anaesthesia) to monitor the wound healing process and prevent unwanted infections. At the first day of wound creation (day 0) and the days when the dressings were changed (days 2 and 4) a biopsy sample of the wounded tissue was collected and snap frozen (similar to what was collected in humans specimen) for

further analysis. At day 4 the animals were sacrificed.

The tissue collected was used primarily to prepare protein lysates for western blot analysis and measurement of enzymatic activities. A similar rat model of acute wound used for NPWT was used to test the efficacy of the MnSOD mimetic, MnE. As a proof of concept design, a single dose of MnE was used based on a previous published work using topical application of MnE to prevent skin carcinogenesis [45] and to match the range of total SOD activity measured in NPWT-treated animals. Briefly, after the administration of isoflurane inhalation to anaesthesize the rats, a 1.5 * 1.5 cm full thickness wound was created under sterile conditions on the animal's back with a surgical blade. After wound creation a volume of 500 µL PBS for the control group or 500 µL MnE (5 µM diluted in PBS) was applied topically at the wound site for 10 min. Following the 10 min incubation a piece of sterile gauze soaked with PBS or MnE solution was applied before applying the dressing. The procedure was then repeated every 2 days for 2 weeks and the wound was monitored each time the dressing was changed. Tissue biopsies were collected only at the beginning and the end of the experiment according to the requirements of analysis. During the dressing changes, the wound was irrigated delicately with 1 mL sterile PBS which was collected back for future analysis of wound fluids. The advancement of wound healing was first assessed through clinical observation of the wound, recording pictures and assessment of different parameters related to wound healing. The “raw” parameters measured in cm^2 related to the wound size were total wound area, open wound area and epithelium area and are illustrated in Fig. S1. These measurements were used to calculate the percentage of wound contraction, percentage of epithelialization and percentage of wound healing using the following formulae commonly used for the assessment of wounds [46,47]:

$$\%\ wound\ contraction = 1 - \left(\frac{Total\ wound\ area\ day_n}{Total\ wound\ area\ day_o}\right)$$

$$\%\ epithelialization = \frac{Epithelium\ area\ day_n}{Total\ wound\ area\ day_n}$$

$$\%\ woundh\ healing = 1 - \left(\frac{Open\ wound\ area\ day_n}{Total\ wound\ area\ day_o}\right)$$

2.3. Electrophoresis and western blot analyses

Tissue extracts (20 µg of proteins) were resolved in 8% or 15% polyacrylamide gels (SDS-PAGE) under denaturing conditions and then transferred to 0.45 µm polyvinylidene difluoride (PVDF) membranes (Millipore) as per the manufacturer's instructions. The membranes were incubated with the relevant primary antibodies anti-Catalase, anti-SOD1, anti-Hif1α (Cell Signaling Technology, Danvers, MA, USA), anti-β-actin (Santa Cruz Biotechnology, Dallas, TX, USA), anti-VEGF, anti-angiopoietin-2 (Abcam, Cambridge, MA, USA), anti-SOD2 (Merck Millipore, Darmstadt, Germany). The bands were visualized using anti-IgG HRP-conjugated secondary antibodies and ECL Western blotting detection system (Amersham Biosciences, UK) and signal acquisition and quantification were performed using iBright Imager and iBright Analysis Software (Thermo Fisher Scientific, Waltham, Massachusetts, USA).

2.4. SOD mimetic

The manganese porphyrine MnE used as an MnSOD mimetic was obtained as 3.96 mM solution in water and prepared as previously described [48]. To obtain a solution of MnE (5 µM) for topical application in the rodent model the stock solution was diluted in PBS and filtered using 0.2 µm filters. The dilution was freshly prepared before each application.

2.5. SOD activity measurement

SOD activity was measured using the SOD assay kit as per the manufacturer instructions (Cayman Chemical, Ann Arbor, Michigan, USA). Briefly SOD activity is measured through its ability to inhibit the oxidation of the soluble tetrazolium salt WSP-1 into a soluble yellow formazan dye by the superoxide produced by recombinant xanthine oxidase [49]. Assay buffer composition is as follows: 50 mM Tris pH 8.0, 0.1 mM hypoxanthine and 0.1 mM diethylenetriaminepentaacetic acid. Reaction inhibition by SOD activity is monitored by measuring absorbance at 460 nm. Bovine recombinant SOD1 was used to generate a standard curve to express the results in mU. Linear rate was calculated for each measure (linear rate = Abs460 for 0 mU of SOD/Abs460 for the tested sample) and then plotted to obtain the correspondent activity (in mU) and normalized per microgram of proteins within the tested sample. Final values are expressed in mU/µg protein.

In order to discriminate between SOD1 and SOD2 activities, 3 mM potassium cyanide (KCN) was added to the assay buffer in order to specifically inhibit SOD1. Absorbance obtained with this condition was then compared to the measure performed without KCN in order to have a specific measure of both SOD activities.

2.6. Antioxidant capacity measurement

Measurement of total antioxidant capacity was performed using the Antioxidant Assay Kit (Cayman Chemical, Ann Arbor, Michigan, USA) according to the manufacturer's manual. The assay is based on the potential of antioxidants within the samples to inhibit the oxidation by metmyoglobin of the substrate 2,2′-azino-di-[3-ethylbenzthiazoline sulphonate] (ABTS) into $ABTS^+$. The total antioxidant capacity in the sample is compared to a standard curve of Trolox, a water-soluble tocopherol analogue, and is quantified as Trolox equivalents (nM/µg of protein).

2.7. Statistical analysis

Each result presented was the result of between 3 and 6 independent experiments. Values measured and represented in graphs are shown as mean ± SEM except for the measurements of effective times for which values are shown as mean ± SD. Two-tail unpaired Student's *t-test* was used when comparing two groups of values. When more than two groups of values were to be compared the statistical analysis was performed using One-way ANOVA followed by *post hoc* Dunnett or Sidak multiple comparison test as indicated in figure legends. P-value < 0,05 was considered significant.

3. Results

3.1. NPWT increases SOD2 protein levels in wound tissue derived from patients

In order to investigate the molecular events involved in redox homeostasis and associated with the improvement of wound healing triggered by NPWT, we first performed an analysis on samples obtained from patients with wounds, before and after the application of NPWT. Patient's tissues were collected from acute wounds such as the one shown in Fig. 1A, Measurement of the total antioxidant capacity of these tissues suggest an overall increase in total antioxidant capacity expressed in Trolox Equivalent after NPWT application as shown in Fig. 1B. Next we performed a western blot analysis of these same samples. First, to validate our experimental settings, we confirmed previously published reports demonstrating that NPWT promotes angiogenesis by increasing VEGF dimer levels at day 2 and day 3 in most of the patient samples tested (Fig. 1C, right panel; Fig. S2) [22,29,50]. Angiopoietin 2, a Tie 2 antagonist and HIF1α target gene, appeared to be normalized or slightly decreasing upon NPWT application at day 2

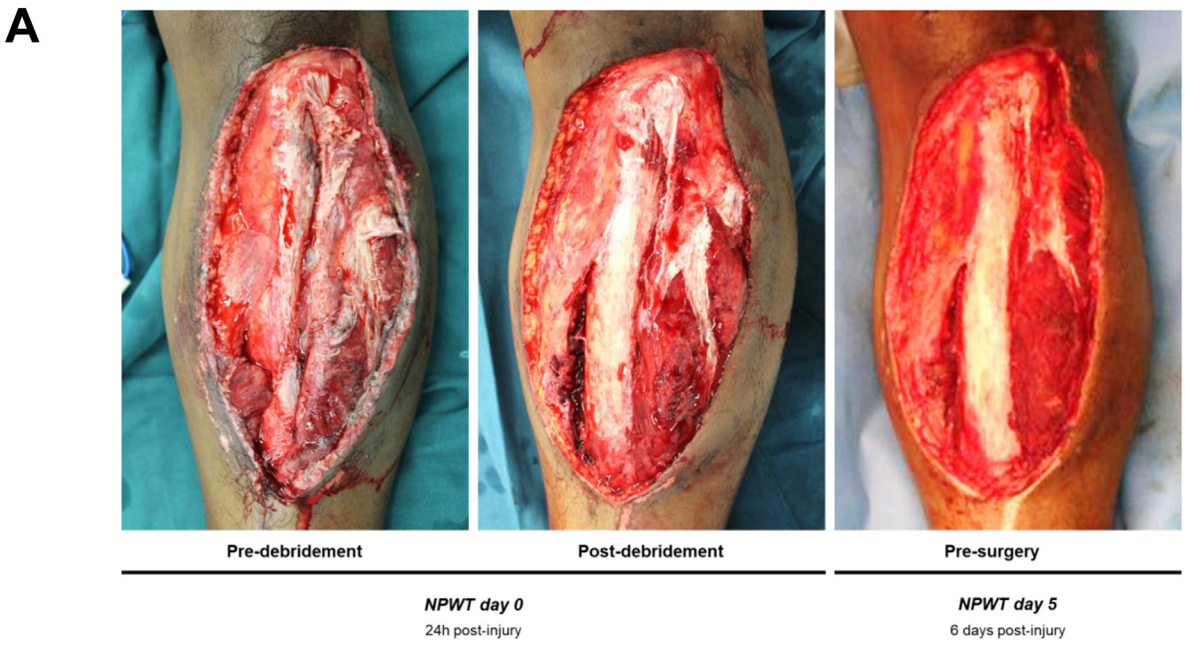

(caption on next page)

Fig. 1. Negative pressure increases total antioxidant capacity and MnSOD protein level in human tissues from wounds treated by NPWT. **A**) Pictures of traumatic wound pre- and post-debridement and after 5 days of NPWT treatment. Deep red granulation tissue formation can be observed following negative pressure application which is one of the main characteristic of this technique. **B**) Measure of total antioxidant capacity (in Trolox equivalent/μg of proteins) in patient samples at day 0 and after 2 and 3 days of NPWT treatment. Statistical analysis performed comparing day 2 and 3 to day 0 using one-way ANOVA followed by post hoc Dunnett multiple comparison test; * $p < 0.05$. **C**) Western blot analysis of patient biopsies at day 0 and after 2 and 3 days of NPWT treatment. Evaluation of the effect of NPWT on NRF2, Catalase, Angiopoietin 2, VEGF (dimer), MnSOD and Cu/ZnSOD with actin used as a loading control. Red lanes outline the main changes observed in patients for NRF2 and MnSOD. Numbers represent individual patients.

(Fig. 1C, left panel) and day 3 (Fig. 1C, right panel), which corroborates previous reports demonstrating that Negative Pressure normalizes the level of hypoxia within the wound bed and alleviates hypoxia signaling [22,23]. Based on our results showing an increase in total antioxidant capacity with NPWT and previous work suggesting the involvement of superoxide dismutases in the wound healing process [34], we checked the levels of SOD1 (Cu/ZnSOD) and SOD2 (MnSOD) in these human samples. While we did not observe a siginficant variation in SOD1 levels, we detected a consistent and reproducible increase in SOD2 levels (Fig. 1C, red lanes; Fig. S2). No significant change in the expression of catalase was observed following NPWT application in patients (Fig. 1C). We also checked the level of NRF2, a major regulator of response to oxidative stress. NRF2 level appeared to be slightly increased in half of the samples tested but not as consistent as the increase in SOD2. These results indicate that NPWT application on human wounds correlates with a regular increase in total antioxidant capacity as well as SOD2 protein level.

3.2. NPWT increases total SOD and SOD2 activities in wound tissues derived from patients

In order to decipher the significance of the increase of SOD2 protein levels in human specimens, we then questioned how it correlated with SOD activity in tissues treated with NPWT. We proceeded to measure SOD activity in the collected samples. We observed that total SOD activity was significantly increased two days after Negative Pressure application on the wounds (Fig. 2A). However, this measurement did not discriminate between SOD1 and SOD2 activities; the relative contribution of SOD1 activity to total SOD activity is much higher than that of SOD2 [49]. In order to assess the level of SOD2 activity, we inhibited SOD1 by adding 3 mM KCN in the enzymatic reaction volume [49], which results in a complete inhibition of SOD1 activity, thus allowing for the specific measurement of SOD2 activity (Fig. 2B). Using this method we then aimed to discriminate between the two enzymes' activities to evaluate if the increase in SOD2 level correlated with an increase in its activity. Notably, Negative Pressure triggered a significant increase in SOD2 activity while SOD1 activity remained relatively unchanged (Fig. 2C). Altogether these results indicate that NPWT triggers an increase of SOD2 activity within the wounded tissue of patients that correlates with an apparent increase in the protein levels.

3.3. NPWT amplifies antioxidant capacity and increases SOD2 protein and activity in a rodent wound model

In order to validate and further investigate the results obtained with the patients' samples, we established a rat model of acute injury based on a previously published protocol [14]. This model allowed us to compare the NPWT-treated group to a control group, which was not possible with the human specimens that we previously collected. Though differences exist between human and rat wound healing mechanisms, the rodent model retains strong similarities that allow quick screening and assays. As seen if Fig. 3A, rats treated with NPWT for 48 h displayed a characteristic increase in granulation tissue formation (black arrow). Mirroring what had been done with the human samples, we measured the total antioxidant capacity of wounded tissues and compared the control and NPWT-treated groups. Results show that, while the total antioxidant capacity of the untreated wounded tissues gradually decreased over time with a significant loss of antioxidant capacity detectable at day 4 (Fig. 3B), the NPWT treated wounds retained a stable antioxidant capacity (Fig. 3B). Moreover, similarly to what was observed in the human samples, angiopoietin 2 levels were significantly lower upon NPWT application compared to the control group (Fig. 3C). VEGF dimer level remained markedly increased with NPWT, although its level was highly induced in the untreated tissues as well (Fig. 3C, Fig S3A and S3B). Hif1α level appeared to be mitigated by NPWT application thus confirming the normalizing effect of negative pressure on hypoxia level and consistent with the trends observed for angiopoietin 2 and VEGF (Fig. 3C; Fig. S3A and S3B). NRF2 appeared to follow a similar pattern with an observed increase in the control groups while their level were reduced or unchanged upon NPWT (Fig. 3C; Fig. S3B). Furthermore, assessment of SOD2 levels revealed a consistent trend in NPWT treated tissues; SOD2 levels increased earlier (day 2) compared to untreated wounds (Fig. 3C, S3B). Together, these results demonstrate that tissues treated with NPWT display normalized levels of hypoxia in the wound site, which in turn could be a link to an improved efficiency of the angiogenesis mechanism, as reported elsewhere [22].

The results obtained with the rodent model corroborate those in human wound specimens, in particular the accumulation of SOD2 in the early stages of wound healing that is significantly observable 48 h after NPWT application. Next, we proceeded to the measurement of SOD activity in the tissues of the animals following NPWT to validate the results obtained with human patients. In the untreated group, total SOD activity dropped steadily between day 0 and day 4 (Fig. 4A, left panel); however, the total SOD activity remained relatively stable when NPWT was applied to the wounds (Fig. 4A, right panel). When KCN was added to discriminate between SOD1 and SOD2 activities, we observed a similar trend to the results found with human patients. SOD1 activity decreased overtime in both control and NPWT groups (Fig. 4B, upper panel); however, SOD2 activity was significantly higher at day 2 and day 4 in the NPWT treated group while no change in activity was observed in the control group (Fig. 4B, lower panel).

3.4. Topical application of SOD2 mimetic hastened wound healing in a rodent-injury model

In view of the results presented above, we postulated that higher SOD2 activity may be one of the key events related to the wound healing enhancement triggered by NPWT. As such, we set out to investigate if the beneficial effects of NPWT could be "replaced" by the topical application of SOD mimetics. To do so, we made use of the SOD2 mimetic, MnE, currently undergoing clinical evaluation and displaying a potent SOD activity (Fig. S4A). Using the aforementioned rodent model of acute injury, MnE (500 μL of 5 μM MnE solution per application) application was used instead of NPWT. MnE was topically applied for 10 min during the change of dressings, every 2 days for 14 days following wound creation (Fig. 5A). A control group was used for comparison with only PBS solution applied on the wound. The wound healing process was monitored and assessed through measurements of standard parameters commonly used in wounded-animal model studies: total wound area (sum of the open wound area + epithelial area), open wound area (representing the area not covered by neo-tissues formed during wound healing) and determination of epithelialization area (total wound area - open wound area) representing the neo-tissue

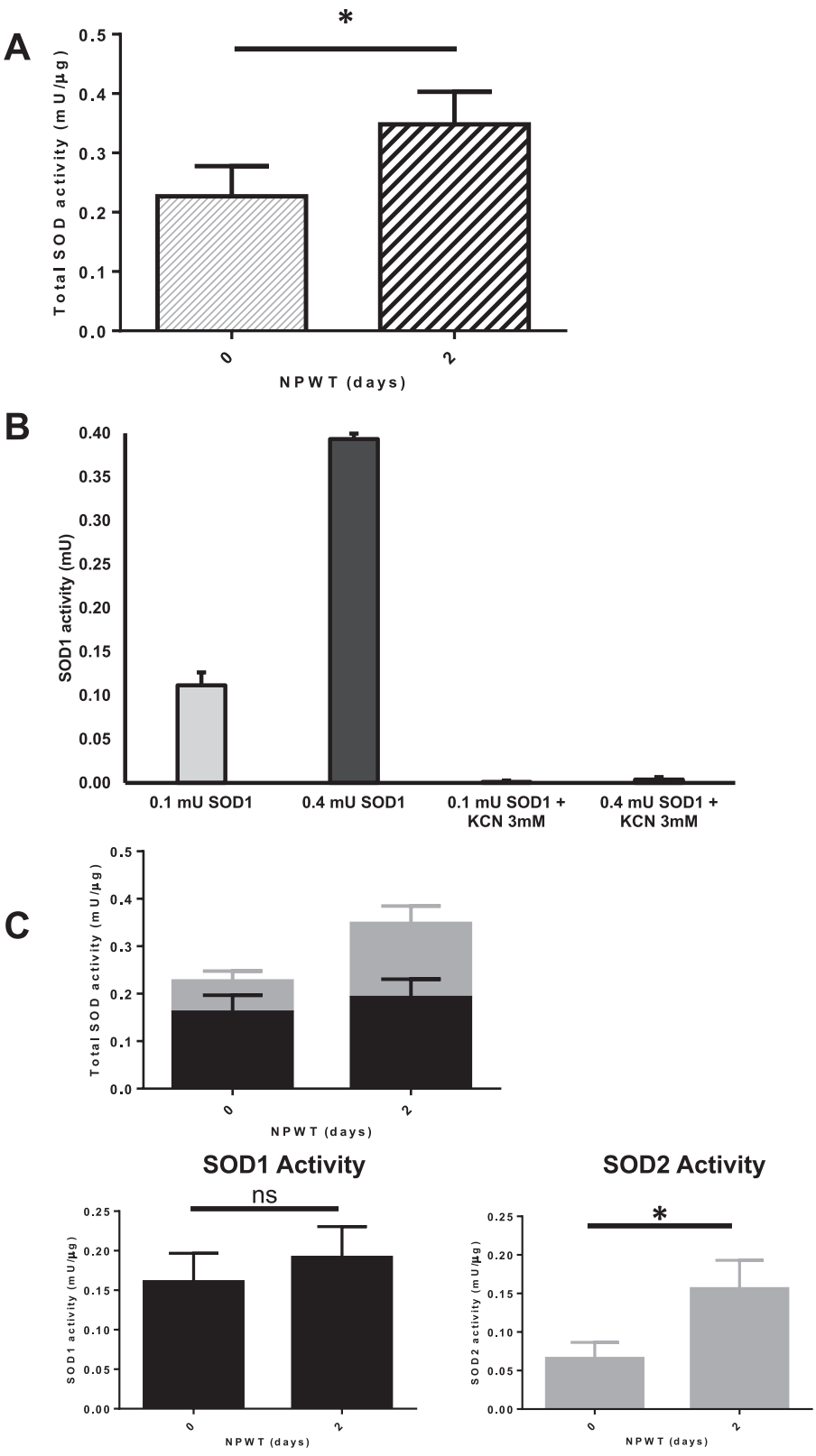

Fig. 2. MnSOD (SOD2) activity is increased in human tissues from wounds following 2 days of NPWT application. **A**) Total SOD activity (in mU/µg of proteins) in patient samples at day 0 and after 2 of negative pressure treatment. *$p < 0.05$. **B**) Validation of the inhibition of Cu/ZnSOD (SOD1) by 3 mM KCN to discriminate between both SOD1 and SOD2 activities. **C**) Discrimination of both SOD1 and SOD2 activities in patient samples at day 0 and after 2 of negative pressure treatment. Total SOD activity as the sum of SOD1 and SOD2 in human biopsies (upper bar graph). SOD1 activity (bottom left bar graph) and SOD2 activity as measured in patient samples at day 0 and after 2 of negative pressure treatment. *$p < 0.05$.

formed during wound healing [46,47]. We observed a visual difference in the kinetics of wound healing between the two groups of animals that was maximal at days 4 and 6, as shown by the size of the open wound area (purple area) shown in Fig. 5B and Fig. S4B. The reduction of the total wound area was not significantly affected by the treatment, though it appeared to decrease slightly faster in the treated than the control group (Fig. 6A). Evaluation of the wound contraction (% wound contraction = 1 − (total wound area day_n/Total wound area day_0)) did not appear to be significantly different between control and treated groups, though once again the contraction seemed to start earlier in the wounds treated with the SOD mimetic (Fig. 6B). However, there were differences between the control and treated groups when the epithelial area composed of neo-tissue formed-to cover and close the wound-was measured, with a significant difference observed at day 6 (Fig. 6C). The

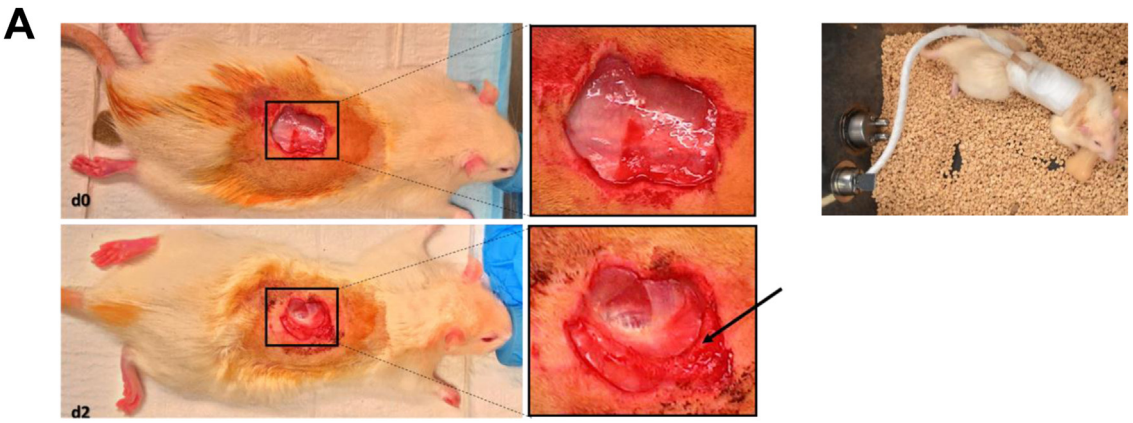

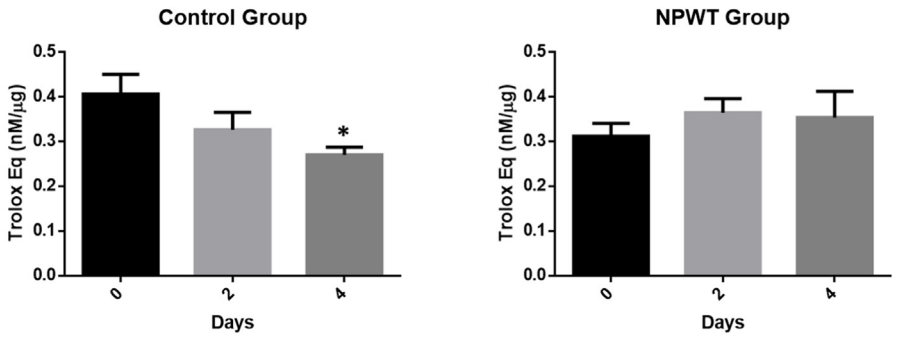

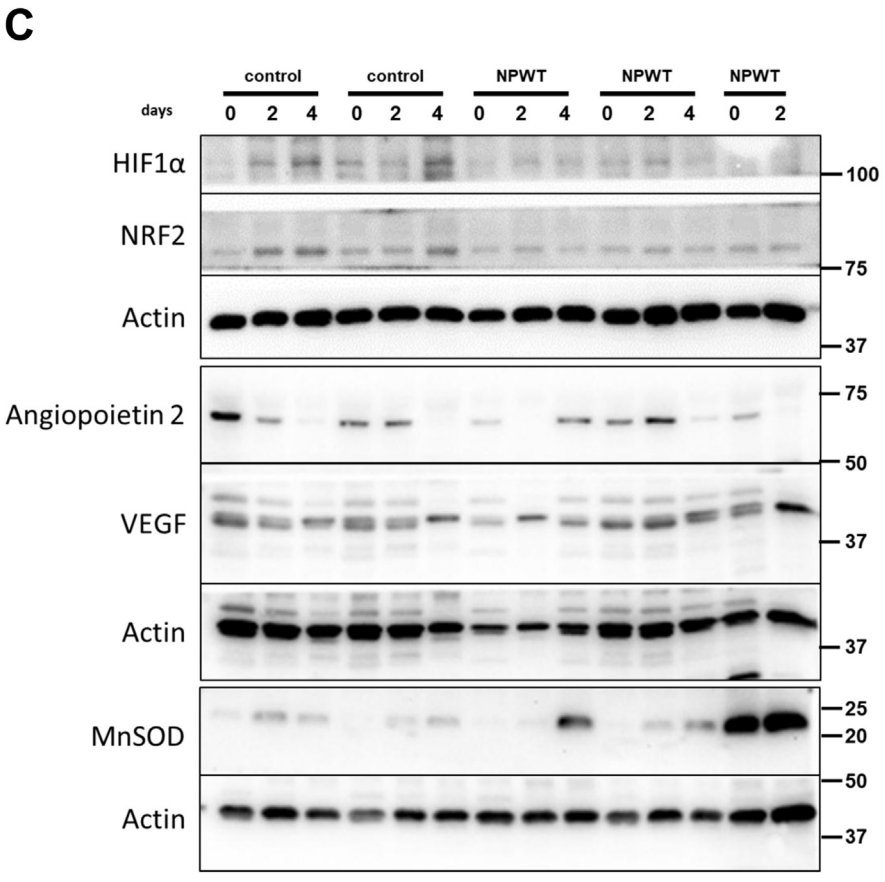

(caption on next page)

Fig. 3. Negative pressure maintains total antioxidant capacity and higher MnSOD protein level in rats treated by NPWT compared to the control rats. **A**) Pictures of surgical wound at day 0 and after 2 days of NPWT treatment. Characteristic granulation tissue formation can be observed following negative pressure application as indicated by the arrow. **B**) Measure of total antioxidant capacity (in Trolox equivalent/μg of proteins) in rat samples at day 0 and after 2 and 4 days in control and NPWT groups. Statistical analysis performed comparing day 2 and 4 to day 0 using one-way ANOVA followed by post hoc Dunnett multiple comparison test; * $p < 0.05$. **C**) Western blot analysis of rat samples from control and NPWT-treated groups at day 0, day 2 and day 4. Evaluation of the effect of NPWT on NRF2, HIF1α, Angiopoietin 2, VEGF (dimer) and MnSOD with actin used as a loading control.

Gaussian shape of the curves representing the epithelized areas in both groups is due to wound contraction occurring after one week with the inflexion point being attributed to the start of the wound contraction. Interestingly, the amount of neo-tissue formed remained similar in both groups, though it is important to note that the kinetics are different with the SOD mimetic treated animals showing the inflexion point occurring about 2 days earlier than for the control group (Fig. 6C). This can be interpreted as the SOD mimetic treatment accelerating neo-tissue formation, thus allowing the wound contraction to start earlier. The assessment of the open-wound area also revealed the positive effect of MnE application, as the open wound area decreased at a faster pace in the treated group with a significant difference at days 4, 6 and 8 compared to the non-treated animals (Fig. 6D). This result favors our previous interpretation that SOD mimetic treatment appears to promote neo-tissue formation within the wound bed.

Further assessment of the wounds was done by calculating the percentage of epithelialization (% Epithelialization = Epithelium area day_n/Total wound area day_n. This evaluation of the impact of MnE application on the neo-tissue formation to fill and close the wounds showed a significant shift in the rate of epithelialization; SOD mimetic treatment hastened the kinetics of tissue formation, covering and closing the open wound with a significant improvement of the

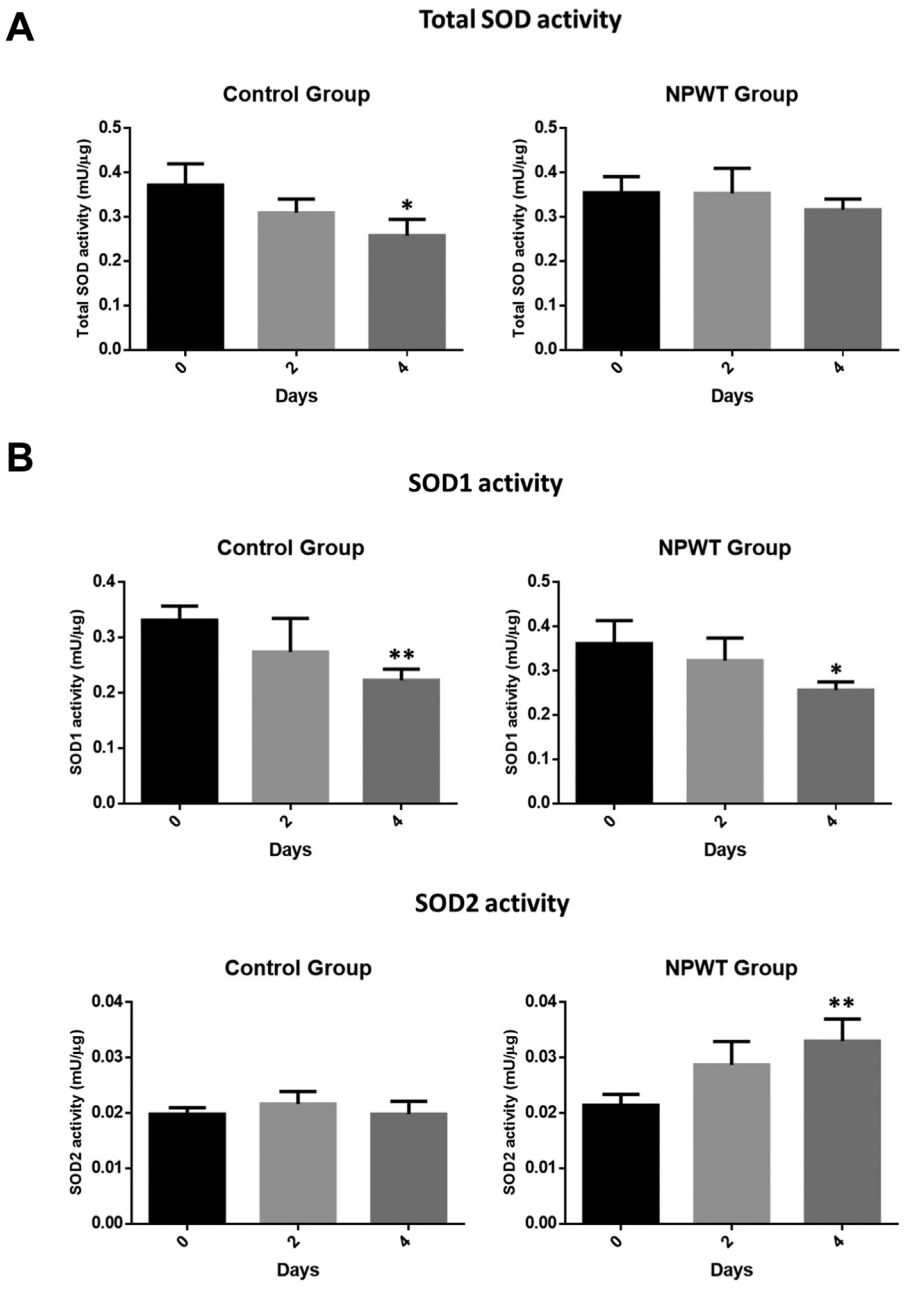

Fig. 4. Negative pressure treatment maintains a higher MnSOD activity level in the NPWT-treated group compared to the control group in the rat model of acute wound. **A**) Total SOD activity (in mU/μg of proteins) in rat samples at day 0 and after 2 and 4 days in control and NPWT groups. Statistical analysis performed comparing day 2 and 4 to day 0 using one-way ANOVA followed by post hoc Dunnett multiple comparison test; * $p < 0.05$. **B**) Measure of SOD1 (upper bar graph) and SOD2 (lower bar graph) activities in rat samples at day 0 and after 2 and 4 days in control and NPWT groups. Statistical analysis performed comparing day 2 and 4 to day 0 using one-way ANOVA followed by post hoc Dunnett multiple comparison test; * $p < 0.05$, * * $p < 0.01$.

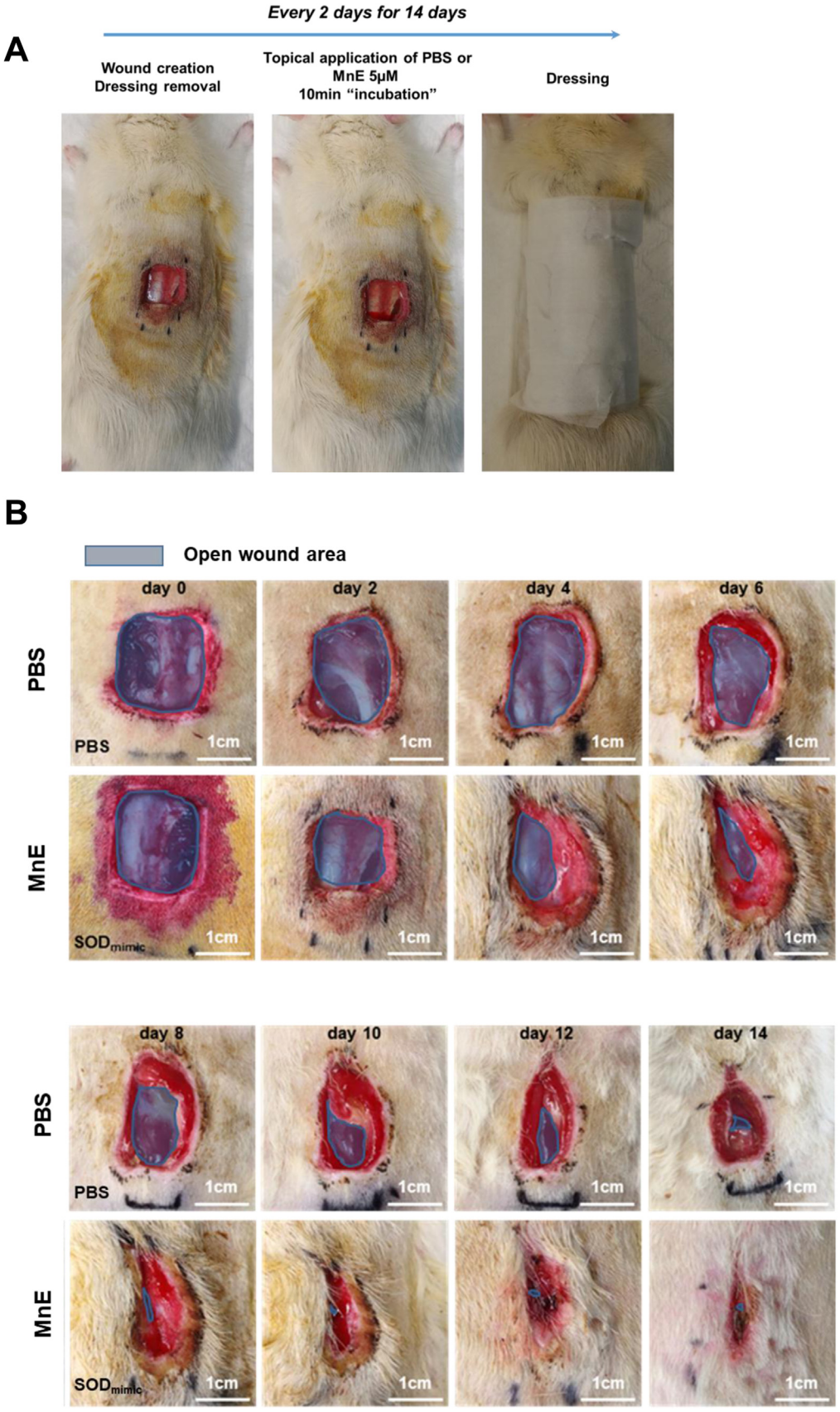

Fig. 5. Replacement of NPWT by the topical application of a MnSOD mimetic (MnE). **A**) Picture of the rodent model of acute wound treated with MnE showing the wound creation step, the topical application of the SOD mimetic and the final dressing. **B**) Pictures of the wounds of 1 representative rat from both control and MnE-treated rats. Pictures were taken every 2 days during dressing change and MnE application. The purple area represents the open wound area as explained in material and methods section and shown in Fig. S1.

A

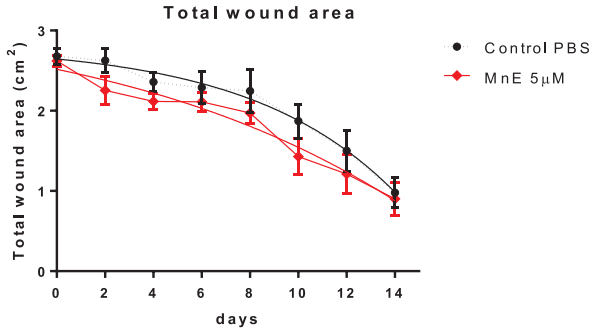

days	Total wound area					
	Control PBS			MnE 5µM		
	mean (cm²)	±SEM	n	mean (cm²)	±SEM	n
0	2.678	0.103	5	2.620	0.072	6
2	2.626	0.155	5	2.253	0.174	6
4	2.360	0.116	5	2.115	0.098	6
6	2.290	0.194	5	2.112	0.119	6
8	2.246	0.270	5	1.970	0.130	6
10	1.872	0.212	5	1.430	0.228	6
12	1.500	0.254	5	1.212	0.246	6
14	0.980	0.192	5	0.900	0.204	6

B

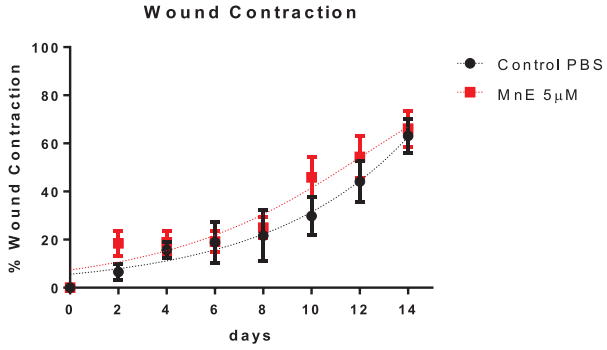

days	Wound contraction					
	Control PBS			MnE 5µM		
	mean (%)	±SEM	n	mean (%)	±SEM	n
0	0.000	0.000	5	0.000	0.000	6
2	6.513	3.257	4	18.490	5.273	5
4	15.685	3.500	4	18.898	4.656	6
6	18.890	8.470	4	19.208	4.409	6
8	21.635	10.525	4	24.937	4.392	6
10	29.760	7.957	5	45.845	8.329	6
12	44.094	8.651	5	54.368	8.631	6
14	63.116	7.101	5	66.110	7.453	6

C

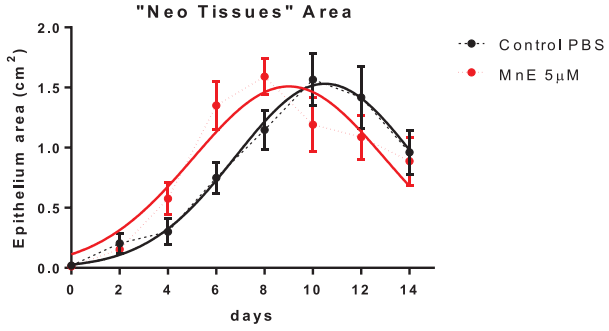

days	Neo tissues area					
	Control PBS			MnE 5µM		
	mean (cm²)	±SEM	n	mean (cm²)	±SEM	n
0	0.020	0.008	5	0.012	0.005	6
2	0.204	0.084	5	0.155	0.022	6
4	0.300	0.108	5	0.577	0.130	6
6	0.750	0.129	5	1.350	0.198	6
8	1.148	0.161	5	1.590	0.151	6
10	1.566	0.217	5	1.192	0.227	6
12	1.418	0.257	5	1.087	0.185	6
14	0.960	0.187	5	0.887	0.200	6

D

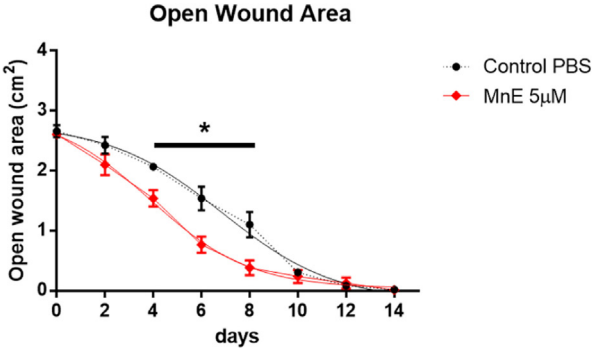

days	Open wound area					
	Control PBS			MnE 5µM		
	mean (cm²)	±SEM	n	mean (cm²)	±SEM	n
0	2.660	0.100	5	2.607	0.075	6
2	2.424	0.143	5	2.098	0.174	6
4	2.064	0.039	5	1.540	0.135	6
6	1.538	0.195	5	0.765	0.134	6
8	1.100	0.213	5	0.382	0.124	6
10	0.306	0.056	5	0.237	0.108	6
12	0.082	0.033	5	0.127	0.090	6
14	0.018	0.012	5	0.012	0.007	6

Fig. 6. MnE treatment promotes wound closure. **A**) Measure of the total wound area over time for both control (PBS) and MnE-treated groups (in cm^2). **B**) Measure of the percentage of wound contraction over time for control and MnE-treated animals. **C**) Measure of the area corresponding to newly formed tissues filling the wound during the wound healing process for control and MnE-treated rats (in cm^2). **D**) Measure of the open wound area in control and MnE-treated rats (in cm^2). Statistical analysis performed comparing control and MnE-treated rats at day n using one-way ANOVA followed by post hoc Sidak multiple comparison test; * $p < 0.05$. Each graph is accompanied by the actual values measured or calculated as explained in the material and methods, SEM and n number of animals (missing n values in percentage of contraction correspond to a "negative contraction" calculated which would not be possible).

A

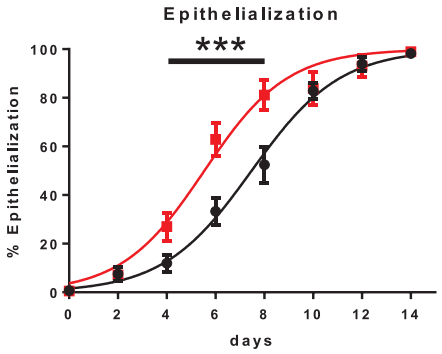

days	Epithelialization					
	Control PBS			MnE 5μM		
	mean (%)	*±SEM*	*n*	*mean (%)*	*±SEM*	*n*
0	0.732	0.233	5	0.515	0.163	6
2	7.564	2.777	5	7.095	1.035	6
4	11.954	3.563	5	27.017	5.816	6
6	33.264	5.729	5	62.868	6.934	6
8	52.476	7.410	5	81.135	6.184	6
10	82.812	3.142	5	83.833	6.871	6
12	93.982	2.888	5	93.040	4.486	6
14	98.220	0.966	5	98.962	0.595	6

B

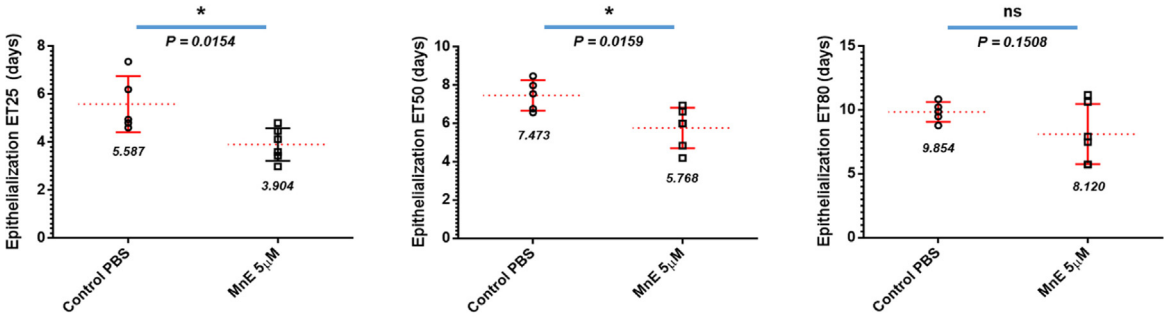

C

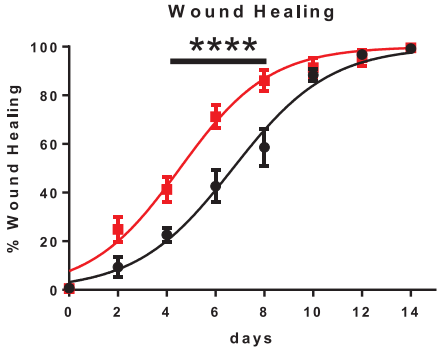

days	Wound Healing					
	Control PBS			MnE 5μM		
	mean (%)	*±SEM*	*n*	*mean (%)*	*±SEM*	*n*
0	0.732	0.233	5	0.515	0.163	6
2	9.416	4.090	5	24.848	5.049	5
4	22.608	2.766	5	41.298	4.996	6
6	42.638	6.707	5	71.233	4.650	6
8	58.620	7.664	5	86.028	4.360	6
10	88.382	2.361	5	91.385	3.848	6
12	96.752	1.506	5	95.432	3.212	6
14	99.186	0.491	5	99.557	0.249	6

D

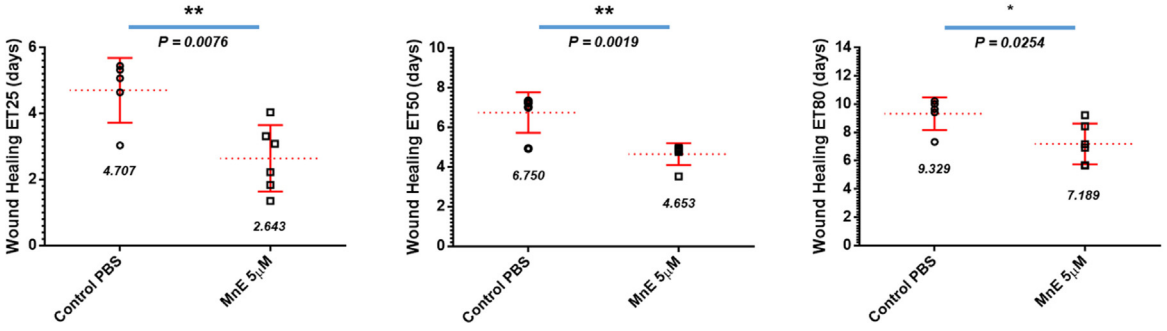

(caption on next page)

Fig. 7. Topical application of MnE accelerates wound healing compared to untreated animals. **A**) Measure of the percentage of epithelialization for both control (PBS) and MnE-treated groups. Statistical analysis performed comparing control and MnE-treated rats at day n using one-way ANOVA followed by post hoc Sidak multiple comparison test; * **p < 0.005. **B**) Estimation of ET25, ET50 and ET80 in control and MnE-treated animals: effective times observed to achieve 25%, 50% and 80% of epithelialization of the wounds respectively. * p < 0.05. **C**) Measure of the percentage of wound healing for both control (PBS) and MnE-treated groups. Statistical analysis performed comparing control and MnE-treated rats at day n using one-way ANOVA followed by post hoc Sidak multiple comparison test; * *** * p < 0.005. **D**) Estimation of ET25, ET50 and ET80 in control and MnE-treated animals: effective times observed to achieve 25%, 50% and 80% of wound healing respectively. * p < 0.05, * *p < 0.01. Graph A and C are accompanied by the actual values for the percentage of epithelialization and wound healing respectively, calculated as explained in the material and methods, with SEM and n number of animals as additional information (remark: the missing value for the second day of MnE treatment was identified as an outlier using the ROUT method and was consequently removed for the accuracy of the analysis).

epithelialization level at day 6 and 8 (Fig. 7A). To further evaluate this effect and the impact of the treatment we measured the effective times necessary to achieve 25%, 50% and 80% of epithelialization for both groups of animals. As shown in Fig. 7B, MnE application significantly decreased ET25 and ET50 (3.904 and 5.768 days, respectively) compared to the untreated group (5.587 and 7.473 days, respectively). No significant difference was observed for ET80 and this was likely due to the wound contraction occurring in rodent models which in turn masked the differences shown at earlier time points (Fig. 7B). These data provide evidence that SOD2 mimetic application accelerates epithelialization of the wound by an average of two days compared to the untreated animals.

Finally, the percentage of wound healing parameter, which represents an evaluation of the wound closure over time following the wound creation (% wound healing = 1- (open wound area day_n/Total wound area day_0), was assessed in response to MnE application. As shown in Fig. 7C the wound closure was significantly and positively affected by MnE treatment. The wound healing percentage curves showed a significant enhancement of the wound closure rate levels at days 4, 6 and 8 following the wound creation (Fig. 7C). We also measured the effective times necessary to achieve 25%, 50% and 80% of wound healing in order to obtain a quantitative estimation of the effect of SOD2 mimetic treatment on the wound closure. These measures showed that the treatment of the wounds with MnE significantly facilitated wound healing as the times required to reach 25%, 50% or 80% of wound closure in the untreated group were 4.707, 6.750 and 9.329 days, respectively, compared to 2.643, 4.653 and 7.189 days, respectively, for the MnE treated group (Fig. 7D). These results indicate that wound closure in the treated group occurred 2 days in advance compared to the control group. Together, these results provide evidence that topical application of SOD2 mimetic promotes neo-epithelium formation and results in accelerated closure of the wound during the first week. These preliminary results highlight the involvement of SOD2 in the various stages of wound healing and underscore the therapeutic potential of SOD2 mimetics in the effective management of acute and/or chronic wounds.

4. Discussion

Wound healing is an important clinical challenge worldwide, and a lot of research has been done in this field in the past decades. Despite the number of published studies, the molecular mechanisms underlying the different phases of wound healing remain insufficiently understood [3,4]. This is due to the complexity of wound healing, which comprises overlapping phases of inflammation, proliferation and remodelling, and the involvement of a multitude of cell types intervening in tissue repair. The intricacy of this system makes it practically impossible to accurately replicate wound healing in an *in vitro* model for deep mechanistic investigations to establish the order, the connections, the overlaps and the redundancy of the molecular mechanisms that have been already described. Far less is known about chronic wounds, even though they are a major preoccupation and burden on the healthcare systems of developed countries [39,51]. Indeed, there is a continued increase in the incidence of chronic wounds due to the combination of an aging population, and associated conditions such as diabetes and vascular disorders, as well as obesity and other metabolic syndromes [6,39,51]. For instance, diabetic foot ulcers are frequently encountered in poorly controlled diabetics, and this in turn can lead to limb amputation [1,6,39,51]. The impaired wound healing observed in diabetes is correlated with a prolonged inflammation phase, a compromised proliferation phase and decreased angiogenesis, which might be partly connected to the high oxidative stress associated with diabetic tissue [37,39]. Many techniques and innovations have been tried in an effort to enhance wound healing, and new ones are continuously being introduced. NPWT, where a dressing is applied to a sealed wound and negative pressure applied to the wound *via* a vacuum device, is one of the techniques used widely in clinical practice. While its clinical benefits are well documented, the mechanisms by which it works are still being elucidated.

In this study we aimed to investigate if antioxidant mechanisms could be regulated by the application of NPWT. Indeed, using patient derived wound tissue, we observed a positive correlation between NPWT and total antioxidant capacity. A consistent increase in the level of SOD2 protein in most of the samples tested was also observed, while no changes were observed for catalase and SOD1. This result correlated with an increase in total SOD activity in clinical tissues upon NPWT for two days, suggesting that negative pressure therapy may influence the antioxidant capacity of wounded tissues. Subsequently, in our attempt to identify the specific SOD isoform responsible for the increase in total activity, we identified SOD2 activity as the major contributor in the augmentation of the anti-oxidant capacity upon NPWT application. Notably, these results were corroborated in a rodent model of acute injury; NPWT helped to maintain a higher antioxidant capacity compared to the control group with significant increases in SOD2 protein level and enzymatic activity. In the animal model, the total SOD activity showed the maintenance of a stable activity in the NPWT treated group compared to the control group. With regards to SOD1, its decrease has been seen in control and NPWT groups over time, while SOD2 activity increases over time in NPWT group.

Interestingly, the difference in total SOD activity increasing over time in human tissues vs stabilizing in rat tissues could be due to the differences in the human and the rat models. The human subjects experienced a delay between the time of injury (wound initiation) and NPWT application, whereas in the case of the rodent model NPWT dressings were applied immediately after the wound creation, which might be the reason for the observed increase in SOD activity in human samples compared to the maintenance of SOD activity in the rodents. It was also reported that SOD1 activity decreases in skin injuries in rats [52] which was confirmed in our rodent model in both control and NPWT groups. Overall, our results highlight the importance of SODs in wound healing triggered by the higher anti-oxidant response elicited upon NPWT.

Since our results showed that NPWT was associated with an increase in SOD2 activity we then attempted to replace NPWT by topical application of a SOD2 mimetic, MnE, which displays high SOD activity, and due to its positive charge localizes to the mitochondria in a way similar to SOD2 [43,44]. We observed that MnE promotes wound healing and advances wound closure by two days in the rodent model. From our observations, the open area of the wound appeared to be covered faster by newly formed tissues in the treated group compared to the non-treated animals. Though it has been observed that SODs may play a role in the early inflammation phase, our results may indicate

that the proliferation phase may also be positively affected by SOD2 mimetic treatment. This is in accordance with a previous study using immobilized SOD1 in hydrogels, which showed improved wound healing and promotion of fibroblast proliferation [53]. In addition, previous reports have demonstrated that SOD2 plays an important role in cell migration and proliferation, crucial mechanisms in skin repair [54,55]. The effect of MnE also helped to confirm an important role of SOD2 in wound healing, as it was previously shown that gene therapy for *Sod2* in a rat model of streptozotocin-induced type I diabetes showed an improvement of the poor wound healing associated with diabetes [56]. Based on these results, we postulate that SOD activity might be an important component in the wound healing process enhanced by NPWT, and that using molecules mimicking SOD activity could represent a promising strategy to promote wound healing. This hypothesis was further supported by previous work showing that diabetes is correlated with diminished SOD2 activity, and that restoration of its expression in endothelial progenitor cells transplanted onto the wounds of diabetic mice restored angiogenesis and wound repair [57].

Finally, many molecules previously tested for their ability to enhance wound healing actually display antioxidant properties [40,41,58]. Using SOD mimetic molecules in chronic wounds has two potential benefits: firstly, it would act as a replacement for a very specific enzymatic activity in wound healing that is impaired, thus restoring a physiological process with a low risk of triggering unwanted side effects. Secondly, it can be used as a tool to unravel the roles of SOD2 activity and ROS modulation in wound healing. Further investigations would be required to decipher the full scope of the role of SODs, and the impact of using SOD mimetics, on wound healing. In particular, the role that SOD2 plays in connecting critical mechanisms such as angiogenesis, hypoxia, metabolic remodelling and fibroblast proliferation/differentiation need further evaluation.

5. Concluding remarks

Our study reports for the first time that NPWT may regulate the antioxidant response of wounded tissues, which in turn correlates with its benefit in wound healing. In addition, we present evidence that SOD activity is a strong inducer of wound healing, as evidenced by the improved wound healing upon the topical application of MnE. This suggests an interesting therapeutic potential for SOD2 mimetics, particularly in the context of non-healing wounds. The use of such molecules in conjunction with NPWT, in particular with the modern systems of NPWT with wound instillation, could also lead to a strong healing effect on recalcitrant wounds.

Acknowledgements

The authors would like to express their gratitude to Jocelyn and Jasmine for their administrative support which has been extremely helpful during the completion of the different steps of this work.

Funding

This work was supported by the National Medical Research Council, Singapore (grant number NMRC/CNIG/1089/2012) and National University Health System (NUHS) Bridging fund (grant number NR15MRF023OM).

Conflict of interest

The authors have no conflict of interest to declare regarded this study.

Appendix A. Supporting information

Supplementary data associated with this article can be found in the online version at doi:10.1016/j.redox.2018.10.014.

References

[1] C.K. Sen, G.M. Gordillo, S. Roy, R. Kirsner, L. Lambert, T.K. Hunt, F. Gottrup, G.C. Gurtner, M.T. Longaker, Human skin woulds: a major and snowballing threat to public health and economy, Wound Repair Regenener. 17 (2019) 763–771, https://doi.org/10.1111/j.1524-475X.2009.00543.x.Human.
[2] K. Järbrink, G. Ni, H. Sönnergren, A. Schmidtchen, C. Pang, R. Bajpai, J. Car, The humanistic and economic burden of chronic wounds: a protocol for a systematic review, Syst. Rev. 6 (2017) 15, https://doi.org/10.1186/s13643-016-0400-8.
[3] T.A. Gray, S. Rhodes, R.A. Atkinson, K. Rothwell, P. Wilson, J.C. Dumville, N.A. Cullum, Opportunities for better value wound care: a multiservice, cross-sectional survey of complex wounds and their care in a UK community population, BMJ Open. 8 (2018), ⟨http://bmjopen.bmj.com/content/8/3/e019440.abstract⟩.
[4] J.F. Guest, K. Vowden, P. Vowden, The health economic burden that acute and chronic wounds impose on an average clinical commissioning group/health board in the UK, J. Wound Care 26 (2017) 292–303, https://doi.org/10.12968/jowc.2017.26.6.292.
[5] B.M. Borena, A. Martens, S.Y. Broeckx, E. Meyer, K. Chiers, L. Duchateau, J.H. Spaas, Regenerative Skin wound healing in mammals: state-of-the-art on growth factor and stem cell based treatments, Cell. Physiol. Biochem. 36 (2015) 1–23, https://doi.org/10.1159/000374049.
[6] R.G. Frykberg, J. Banks, Challenges in the treatment of chronic wounds, Adv. Wound Care 4 (2015) 560–582, https://doi.org/10.1089/wound.2015.0635.
[7] G. Gurtner, S. Werner, Y. Barrandon, M. Longaker, Wound repair and regeneration, Nature 453 (2008) 314–321, https://doi.org/10.1038/nature07039.
[8] J.M. Reinke, H. Sorg, Wound repair and regeneration, Eur. Surg. Res. 49 (2012) 3543, https://doi.org/10.1159/000339613.
[9] M.S. Hu, G.G. Walmsley, L.A. Barnes, K. Weiskopf, R.C. Rennert, D. Duscher, M. Januszyk, Z.N. Maan, W.X. Hong, A.T.M. Cheung, T. Leavitt, C.D. Marshall, R.C. Ransom, S. Malhotra, A.L. Moore, J. Rajadas, H.P. Lorenz, I.L. Weissman, G.C. Gurtner, M.T. Longaker, Delivery of monocyte lineage cells in a biomimetic scaffold enhances tissue repair, JCI Insight 2 (2017), https://doi.org/10.1172/jci.insight.96260.
[10] V.W. Wong, J.D. Crawford, Vasculogenic cytokines in wound healing, Biomed. Res. Int. 2013 (2013), https://doi.org/10.1155/2013/190486.
[11] A. Sood, M.S. Granick, N.L. Tomaselli, Wound dressings and comparative effectiveness data, Adv. Wound Care 3 (2014) 511–529, https://doi.org/10.1089/wound.2012.0401.
[12] K. Harding, Innovation and wound healing, J. Wound Care 24 (2015) 7–13, https://doi.org/10.12968/jowc.2015.24.Sup4b.7.
[13] S. Lalezari, C.J. Lee, A.A. Borovikova, D.A. Banyard, K.Z. Paydar, G.A. Wirth, A.D. Widgerow, Deconstructing negative pressure wound therapy, Int. Wound J. (2016) 1–9, https://doi.org/10.1111/iwj.12658.
[14] S. Jacobs, D.A. Simhaee, A. Marsano, G.M. Fomovsky, G. Niedt, J.K. Wu, Efficacy and mechanisms of vacuum-assisted closure (VAC) therapy in promoting wound healing: a rodent model, J. Plast. Reconstr. Aesthetic Surg. 62 (2009) 1331–1338, https://doi.org/10.1016/j.bjps.2008.03.024.
[15] C.S. Garwood, J.S. Steinberg, What's new in wound treatment: a critical appraisal, Diabetes Metab. Res. Rev. 32 (2016) 268–274, https://doi.org/10.1002/dmrr.2747.
[16] M.Y. Hasan, R. Teo, A. Nather, Negative-pressure wound therapy for management of diabetic foot wounds: a review of the mechanism of action, clinical applications, and recent developments, Diabet. Foot Ankle 6 (2015), https://doi.org/10.3402/dfa.v6.27618.
[17] A. Nather, S.B. Chionh, A.Y.Y. Han, P.P.L. Chan, A. Nambiar, Effectiveness of vacuum-assisted closure (VAC) therapy in the healing of chronic diabetic foot ulcers, Ann. Acad. Med. Singap. 39 (2010) 353–358.
[18] C.M. Mouës, F. Heule, S.E.R. Hovius, A review of topical negative pressure therapy in wound healing: sufficient evidence? Am. J. Surg. 201 (2011) 544–556, https://doi.org/10.1016/j.amjsurg.2010.04.029.
[19] P.S. Murphy, G.R.D. Evans, Advances in wound healing: a review of current wound healing products, Plast. Surg. Int. 2012 (2012) 1–8, https://doi.org/10.1155/2012/190436.
[20] C. Wiegand, R. White, Microdeformation in wound healing, Wound Repair Regener. (2013) 793–799, https://doi.org/10.1111/wrr.12111.
[21] C.Y. Xia, A.X. Yu, B. Qi, M. Zhou, Z.H. Li, W.Y. Wang, Analysis of blood flow and local expression of angiogenesis-associated growth factors in infected wounds treated with negative pressure wound therapy, Mol. Med. Rep. 9 (2014) 1749–1754, https://doi.org/10.3892/mmr.2014.1997.
[22] P. Erba, R. Ogawa, M. Ackermann, A. Adini, L.F. Miele, P. Dastouri, D. Helm, S.J. Mentzer, R.J. D'Amato, G.F. Murphy, M.A. Konerding, D.P. Orgill, Angiogenesis in wounds treated by microdeformational wound therapy, Ann. Surg. 253 (2011) 402–409, https://doi.org/10.1097/SLA.0b013e31820563a8.
[23] A. Grimm, A. Dimmler, S. Stange, A. Labanaris, R. Sauer, G. Grabenbauer, R.E. Horch, Expression of HIF-1α In irradiated tissue is altered by topical negative-pressure therapy, Strahlenther. Und Onkol. 183 (2007) 144–149, https://doi.org/10.1007/s00066-007-1560-1.
[24] W. Wang, Z. Pan, X. Hu, Z. Li, Y. Zhao, A.X. Yu, Vacuum-assisted closure increases ICAM-1, MIF, VEGF and collagen I expression in wound therapy, Exp. Ther. Med. 7 (2014) 1221–1226, https://doi.org/10.3892/etm.2014.1567.
[25] D.P. Orgill, E.K. Manders, B.E. Sumpio, R.C. Lee, C.E. Attinger, G.C. Gurtner, H.P. Ehrlich, The mechanisms of action of vacuum assisted closure: more to learn, Surgery 146 (2009) 40–51, https://doi.org/10.1016/j.surg.2009.02.002.

[26] L. Lancerotto, L.R. Bayer, D.P. Orgill, Mechanisms of action of microdeformational wound therapy, Semin. Cell Dev. Biol. 23 (2012) 987–992, https://doi.org/10.1016/j.semcdb.2012.09.009.
[27] V. Saxena, C.W. Hwang, S. Huang, Q. Eichbaum, D. Ingber, D.P. Orgill, Vacuum-assisted closure: microdeformations of wounds and cell proliferation, Plast. Reconstr. Surg. 114 (2004) 1086–1096, https://doi.org/10.1097/01.PRS.0000135330.51408.97.
[28] S.-L. Yang, R. Han, Y. Liu, L.-Y. Hu, X.-L. Li, L.-Y. Zhu, Negative pressure wound therapy is associated with up-regulation of bFGF and ERK1/2 in human diabetic foot wounds, Wound Repair Regener. 22 (2014) 548–554, https://doi.org/10.1111/wrr.12195.
[29] F. Lu, R. Ogawa, D.T. Nguyen, B. Chen, D. Guo, D.L. Helm, Q. Zhan, G.F. Murphy, D.P. Orgill, Microdeformation of three-dimensional cultured fibroblasts induces gene expression and morphological changes, Ann. Plast. Surg. 66 (2011) 296–300, https://doi.org/10.1097/SAP.0b013e3181ea1e9b.
[30] K.E. Johnson, T.A. Wilgus, Vascular endothelial growth factor and angiogenesis in the regulation of cutaneous wound repair, Adv. Wound Care 3 (2014) 647–661, https://doi.org/10.1089/wound.2013.0517.
[31] E. Anesäter, O. Borgquist, E. Hedström, J. Waga, R. Ingemansson, M. Malmsjö, The influence of different sizes and types of wound fillers on wound contraction and tissue pressure during negative pressure wound therapy, Int. Wound J. 8 (2011) 336–342, https://doi.org/10.1111/j.1742-481X.2011.00790.x.
[32] N. Kairinos, M. Solomons, D.A. Hudson, Negative-pressure wound therapy I: the paradox of negative-pressure wound therapy, Plast. Reconstr. Surg. 123 (2009), ⟨https://journals.lww.com/plasreconsurg/Fulltext/2009/02000/Negative_Pressure_Wound_Therapy_I__The_Paradox_of.19.aspx⟩.
[33] F. Peinemann, S. Sauerland, Negative-pressure wound therapy: systematic review of randomized controlled trials, Dtsch. Arztebl. Int. 108 (2011) 381–389, https://doi.org/10.3238/arztebl.2011.0381.
[34] T. Kurahashi, J. Fujii, Roles of antioxidative enzymes in wound healing, J. Dev. Biol. 3 (2015) 57–70, https://doi.org/10.3390/jdb3020057.
[35] T.K. Hunt, R.S. Aslam, S. Beckert, S. Wagner, Q.P. Ghani, M.Z. Hussain, S. Roy, C.K. Sen, Aerobically derived lactate stimulates revascularization and tissue repair *via* redox mechanisms, Antioxid. Redox Signal. 9 (2007) 1115–1124, https://doi.org/10.1089/ars.2007.1674.
[36] M. Schäfer, S. Werner, Oxidative stress in normal and impaired wound repair, Pharmacol. Res. 58 (2008) 165–171, https://doi.org/10.1016/j.phrs.2008.06.004.
[37] C.K. Sen, S. Khanna, G. Gordillo, D. Bagchi, M. Bagchi, S. Roy, Oxygen, oxidants, and antioxidants in wound healing: an emerging paradigm, Ann. N. Y. Acad. Sci. 957 (2002) 239–249, https://doi.org/10.1111/j.1749-6632.2002.tb02920.x.
[38] O. Trabold, S. Wagner, C. Wicke, H. Scheuenstuhl, M.Z. Hussain, N. Rosen, A. Seremetiev, H.D. Becker, T.K. Hunt, Lactate and oxygen constitute a fundamental regulatory mechanism in wound healing, Wound Repair Regen. 11 (2003) 504–509, https://doi.org/10.1046/j.1524-475X.2003.11621.x.
[39] K. Anderson, R.L. Hamm, Factors that impair wound healing, J. Am. Coll. Clin. Wound Spec. 4 (2012) 84–91, https://doi.org/10.1016/j.jccw.2014.03.001.
[40] R.S.S. Barreto, R.L.C. Albuquerque-Júnior, A.A.S. Araújo, J.R.G.S. Almeida, M.R.V. Santos, A.S. Barreto, J.M. DeSantana, P.S. Siqueira-Lima, J.S.S. Quintans, L.J. Quintans-Júnior, A systematic review of the wound-healing effects of monoterpenes and iridoid derivatives, Molecules 19 (2014) 846–862, https://doi.org/10.3390/molecules19010846.
[41] G. Mao, M. Goswami, A.L. Kalen, P.C. Goswami, E.H. Sarsour, N-acetyl-L-cysteine increases MnSOD activity and enhances the recruitment of quiescent human fibroblasts to the proliferation cycle during wound healing, Mol. Biol. Rep. 43 (2016) 31–39, https://doi.org/10.1007/s11033-015-3935-1.
[42] I. Batinic-Haberle, I. Spasojevic, Complex chemistry and biology of redox-active compounds, commonly known as SOD mimics, affect their therapeutic effects, Antioxid. Redox Signal. 20 (2014) 2323–2325, https://doi.org/10.1089/ars.2014.5921.
[43] S. Miriyala, I. Spasojevic, A. Tovmasyan, D. Salvemini, Z. Vujaskovic, D. St Clair, I. Batinic-Haberle, Manganese superoxide dismutase, MnSOD and its mimics, Biochim. Biophys. Acta 1822 (2012) 794–814, https://doi.org/10.1016/j.bbadis.2011.12.002 ⟨doi:⟩.
[44] A.M. Li, J. Martins, A. Tovmasyan, J.S. Valentine, I. Batinic-Haberle, I. Spasojevic, E.B. Gralla, Differential localization and potency of manganese porphyrin superoxide dismutase-mimicking compounds in Saccharomyces cerevisiae, Redox Biol. 3 (2014) 1–6, https://doi.org/10.1016/j.redox.2014.09.003.
[45] Y. Zhao, L. Chaiswing, T.D. Oberley, I. Batinic-Haberle, W. St Clair, C.J. Epstein, D. St Clair, A mechanism-based antioxidant approach for the reduction of skin carcinogenesis, Cancer Res. 65 (2005) 1401–1405, https://doi.org/10.1158/0008-5472.CAN-04-3334.
[46] M.W. Bohling, R.A. Henderson, S.F. Swaim, S.A. Kincaid, J.C. Wright, Cutaneous wound healing in the cat: a macroscopic description and comparison with cutaneous wound healing in the dog, Vet. Surg. 33 (2004) 579–587, https://doi.org/10.1111/j.1532-950X.2004.04081.x.
[47] L. Chen, E.E. Tredget, P.Y.G. Wu, Y. Wu, Y. Wu, Paracrine factors of mesenchymal stem cells recruit macrophages and endothelial lineage cells and enhance wound healing, PLoS One 3 (2008), https://doi.org/10.1371/journal.pone.0001886.
[48] I. Batinić-Haberle, I. Spasojević, P. Hambright, L. Benov, A.L. Crumbliss, I. Fridovich, Relationship among redox potentials, proton dissociation constants of Pyrrolic Nitrogens, and in vivo and in vitro superoxide dismutating activities of Manganese(III) and Iron(III) water-soluble porphyrins, Inorg. Chem. 38 (1999) 4011–4022, https://doi.org/10.1021/ic990118k.
[49] A.V. Peskin, C.C. Winterbourn, Assay of superoxide dismutase activity in a plate assay using WST-1, Free Radic. Biol. Med. 103 (2017) 188–191, https://doi.org/10.1016/j.freeradbiomed.2016.12.033.
[50] L. Morbidelli, R. Birkenhaeger, W. Roeckl, H.J. Granger, U. Kaerst, H.A. Weich, M. Ziche, Distinct capillary density and progression promoted by vascular endothelial growth factor-A homodimers and heterodimers, Angiogenesis 1 (1997) 117–130, https://doi.org/10.1023/A:1018361217467.
[51] S. Guo, L.A. DiPietro, Factors affecting wound healing, J. Dent. Res. 89 (2010) 219–229, https://doi.org/10.1177/0022034509359125.
[52] A. Shukla, A.M. Rasik, G.K. Patnaik, Depletion of reduced glutathione, ascorbic acid, vitamin E and antioxidant defence enzymes in a healing cutaneous wound, Free Radic. Res. 26 (1997) 93–101, https://doi.org/10.3109/10715769709097788.
[53] A. Chiumiento, S. Lamponi, R. Barbucci, A. Domínguez, Y. Pérez, R. Villalonga, Immobilizing Cu, Zn-superoxide dismutase in hydrogels of carboxymethylcellulose improves its stability and wound healing properties, Biochem. Biokhimiia 71 (2006) 1324–1328, https://doi.org/10.1134/S0006297906120066.
[54] A.P. Kumar, S.Y. Loo, S.W. Shin, T.Z. Tan, C.B. Eng, R. Singh, T.C. Putti, C.W. Ong, M. Salto-Tellez, B.C. Goh, J.I. Park, J.P. Thiery, S. Pervaiz, M.V. Clement, Manganese superoxide dismutase is a promising target for enhancing chemosensitivity of basal-like breast carcinoma, Antioxid. Redox Signal. 20 (2014) 2326–2346, https://doi.org/10.1089/ars.2013.5295.
[55] S.Y. Loo, J.L. Hirpara, V. Pandey, T.Z. Tan, C.T. Yap, P.E. Lobie, J.P. Thiery, B.C. Goh, S. Pervaiz, M.-V. Clément, A.P. Kumar, Manganese superoxide dismutase expression regulates the switch between an epithelial and a mesenchymal-like phenotype in breast carcinoma, Antioxid. Redox Signal. 25 (2016) 283–299, https://doi.org/10.1089/ars.2015.6524.
[56] J.-D. Luo, Y.-Y. Wang, W.-L. Fu, J. Wu, A.F. Chen, Gene therapy of endothelial nitric oxide synthase and manganese superoxide dismutase restores delayed wound healing in type 1 diabetic mice, Circulation 110 (2004) 2484–2493, https://doi.org/10.1161/01.CIR.0000137969.87365.05.
[57] E.J. Marrotte, D.-D. Chen, J.S. Hakim, A.F. Chen, Manganese superoxide dismutase expression in endothelial progenitor cells accelerates wound healing in diabetic mice, J. Clin. Investig. 120 (2010) 4207–4219, https://doi.org/10.1172/JCI36858.
[58] R.F. Pereira, P.J. Bártolo, Traditional therapies for skin wound healing, Adv. Wound Care 5 (2016) 208–229, https://doi.org/10.1089/wound.2013.0506.